JACC: CARDIOVASCULAR IMAGING VOL. 13, NO. 3, 2020

PUBLISHED BY ELSEVIER

ORIGINAL RESEARCH

Cardiac Magnetic Resonance for Evaluating Nonculprit Lesions After Myocardial Infarction

Comparison With Fractional Flow Reserve

Henk Everaars, MD,[a,*] Nina W. van der Hoeven, MD,[a,*] Gladys N. Janssens, MD,[a] Maarten A. van Leeuwen, MD,[e] Ramon B. van Loon, MD, PhD,[a] Stefan P. Schumacher, MD,[a] Ahmet Demirkiran, MD,[a] Mark B.M. Hofman, PhD,[c] Rob J. van der Geest, PhD,[d] Peter M. van de Ven, PhD,[b] Marco J. Götte, MD, PhD,[a] Albert C. van Rossum, MD, PhD,[a] Niels van Royen, MD, PhD,[a,f] Robin Nijveldt, MD, PhD[a,f]

ABSTRACT

OBJECTIVES This study sought to determine the agreement between cardiac magnetic resonance (CMR) imaging and invasive measurements of fractional flow reserve (FFR) in the evaluation of nonculprit lesions after ST-segment elevation myocardial infarction (STEMI). In addition, we investigated whether fully quantitative analysis of myocardial perfusion is superior to semiquantitative and visual analysis.

BACKGROUND The agreement between CMR and FFR in the evaluation of nonculprit lesions in patients with STEMI with multivessel disease is unknown.

METHODS Seventy-seven patients with STEMI with at least 1 intermediate (diameter stenosis 50% to 90%) nonculprit lesion underwent CMR and invasive coronary angiography in conjunction with FFR measurements at 1 month after primary intervention. The imaging protocol included stress and rest perfusion, cine imaging, and late gadolinium enhancement. Fully quantitative, semiquantitative, and visual analysis of myocardial perfusion were compared against a reference of FFR. Hemodynamically obstructive was defined as FFR $\leq$0.80.

RESULTS Hemodynamically obstructive nonculprit lesions were present in 31 (40%) patients. Visual analysis displayed an area under the curve (AUC) of 0.74 (95% confidence interval [CI]: 0.62 to 0.83), with a sensitivity of 73% and a specificity of 70%. For semiquantitative analysis, the relative upslope of the stress signal intensity time curve and the relative upslope derived myocardial flow reserve had respective AUCs of 0.66 (95% CI: 0.54 to 0.77) and 0.71 (95% CI: 0.59 to 0.81). Fully quantitative analysis did not augment diagnostic performance (all $p > 0.05$). Stress myocardial blood flow displayed an AUC of 0.76 (95% CI: 0.64 to 0.85), with a sensitivity of 69% and a specificity of 77%. Similarly, MFR displayed an AUC of 0.82 (95% CI: 0.71 to 0.90), with a sensitivity of 82% and a specificity of 71%.

CONCLUSIONS CMR and FFR have moderate-good agreement in the evaluation of nonculprit lesions in patients with STEMI with multivessel disease. Fully quantitative, semiquantitative, and visual analysis yield similar diagnostic performance. (J Am Coll Cardiol Img 2020;13:715-28) © 2020 by the American College of Cardiology Foundation.

From the [a]Department of Cardiology, Amsterdam University Medical Centers, location VUmc, Amsterdam, the Netherlands; [b]Department of Epidemiology and Biostatistics, Amsterdam University Medical Centers, Amsterdam, the Netherlands; [c]Department of Radiology and Nuclear Medicine, Amsterdam UMC, Amsterdam, the Netherlands; [d]Department of Radiology, Leiden University Medical Center, Leiden, the Netherlands; [e]Department of Cardiology, Isala Clinics, Zwolle, the Netherlands; and the [f]Department of Cardiology, Radboud University Medical Centers, Nijmegen, the Netherlands. *Drs. Everaars and van der Hoeven contributed equally to this manuscript. This is a substudy of the REDUCE-MVI trial, which was initiated by the Amsterdam UMC, Amsterdam, the Netherlands, with financial support from AstraZeneca through an unrestricted research grant. In addition, the study was financed by the Ministry of Economic Affairs of the Netherlands by means of a PPP Allowance

ISSN 1936-878X/$36.00 https://doi.org/10.1016/j.jcmg.2019.07.019

ABBREVIATIONS AND ACRONYMS

AUC = area under the curve

CAD = coronary artery disease

CI = confidence interval

CFR_{thermo} = thermodilution derived coronary flow reserve

CMR = cardiac magnetic resonance

FFR = fractional flow reserve

IMR = index of microcirculatory resistance

LGE = late gadolinium enhancement

MBF = myocardial blood flow

MFR = myocardial flow reserve

MFR rel upslope = myocardial flow reserve relative upslope derived flow reserve

ROC = receiver-operator characteristic

stress rel upslope = stress signal intensity time curve

SAQ = Seattle angina questionnaire

STEMI = ST-segment elevation myocardial infarction

Over the past few decades, cardiac magnetic resonance (CMR) imaging has emerged as a robust tool to evaluate patients with suspected obstructive coronary artery disease (CAD). Among the myriad of imaging techniques, CMR has the advantages of being cost-effective (1), widely available, and multiparametric (i.e., it allows to evaluate several pathological features during a single session). In addition, CMR does not expose patients to ionizing radiation while permitting imaging at high spatial resolution. Finally, patients with normal CMR results have a reassuring low risk of future cardiovascular events (2).

SEE PAGE 729

In the clinical setting, perfusion images are typically assessed visually; however, CMR can also quantify myocardial blood flow (MBF) in relative (semiquantitative) (3) and even absolute terms (fully quantitative) (4). Conflicting evidence exists as to whether quantification improves the diagnostic accuracy of perfusion CMR. Although some studies reported superiority of fully quantitative analysis over semiquantitative and visual analysis (5), others found no benefit of quantification in the diagnosis of obstructive CAD (6–8). In patients with stable CAD, invasive measurements of fractional flow reserve (FFR) are considered the optimal index for diagnosing hemodynamically obstructive CAD and guiding revascularization (9). Although CMR and FFR are reported to have a high concordance in the assessment of patients with stable CAD (10), the agreement between CMR and FFR in the evaluation of nonculprit lesions after ST-segment elevation myocardial infarction (STEMI) is still unknown. Nonculprit lesions are present in approximately 50% of patients with STEMI and, if left unattended, carry a poor prognosis (11,12). In these patients, CMR is of special interest as it allows for simultaneous assessment of left ventricular function, infarction size, and perfusion. CMR thus not only provides valuable prognostic information, but also identifies patients with ischemia in nonculprit vascular territories who may benefit from revascularization.

The aim of the present study was to determine the agreement between CMR and invasive measurements of FFR in the evaluation of nonculprit lesions in patients with STEMI with multivessel disease. Visual assessment of myocardial perfusion images was compared to semi- and fully quantitative analysis.

METHODS

STUDY POPULATION. This is a substudy of data from patients enrolled in the REDUCE-MVI (Reducing Micro Vascular Dysfunction in Acute Myocardial Infarction by Ticagrelor) trial in the Amsterdam UMC, location VUmc. The main results of this trial have been published previously (13). Briefly, patients with a first STEMI and at least 1 intermediate lesion in a nonculprit vessel were enrolled after successful revascularization of the culprit. Intermediate was defined as 50% to 90% diameter stenosis. The main exclusion criteria were cardiogenic shock, decompensated heart failure, left main disease, and chronic total occlusion. Acute STEMI management and subsequent medical care followed contemporary guidelines (14). Follow-up CMR and invasive assessment were scheduled 1 month after the index event. CMR always preceded invasive assessment. Patients were instructed to refrain from products containing caffeine or xanthine for 24 h before the follow-up visit. To evaluate angina burden, patients completed the Seattle Angina Questionnaire (SAQ) upon arrival at the hospital (15). The study protocol was approved by the institutional review committee of the Amsterdam UMC, location VUmc. All patients gave written informed consent.

CMR IMAGE ACQUISITION. All images were obtained on a 1.5-T clinical scanner (Magnetom Avanto, Siemens Healthineers, Erlangen, Germany). Perfusion imaging was performed using a dual-sequence technique (16). High-resolution images of myocardial perfusion were acquired using an echo planar

made available by the Top Sector Life Sciences & Health to stimulate public-private partnerships. The funding sources did not have any role in the study design; collection, analysis, or interpretation of data; preparation of the manuscript; or decision to submit it for publication. Dr. van Royen reports research grants from AstraZeneca, Abbott, Philips, Biotronik, and Top Sector Life Sciences & Health during the conduct of the study. Dr. van Leeuwen has received research grants from AstraZeneca. Dr. Nijveldt has received research grants from Philips and Biotronik; and financial support from the Netherlands Organization for Health Research and Development (grant 9071544). Dr. Demirkiran has received a research grant from the postdoctoral international research fellowship program of the Scientific and Technological Research Council of Turkey (ref: 53325897-115.02-170549). All other authors have reported that they have no relationships relevant to the contents of this paper to disclose.

Manuscript received May 28, 2019; accepted July 10, 2019.

imaging sequence in 3 parallel short-axis slices planned at the basal, mid and apical levels. To assess the arterial input function, low-resolution turboFLASH images were acquired at the basal level using a sequence optimized for the high gadolinium concentration. Perfusion images were obtained every heartbeat for 50 to 70 cardiac cycles following intravenous injection of a 0.075 mmol/kg bolus of a gadolinium-based contrast agent (DOTAREM, Guerbet, Villepinte, France). In-plane respiratory motion of the heart was corrected using a nonrigid registration (17). Perfusion images were corrected for surface coil induced inhomogeneities through a separate prescan normalization (18). Typical in-plane resolution of the myocardial perfusion images was 2.5 × 2.5 mm, with a slice thickness of 10 mm (prepulse 90°, repetition time 5.6 ms, echo time 1.1 ms, saturation time 110 ms, flip angle 18°, matrix 144 × 160). Stress was induced by continuous infusion of adenosine at 140 μg/kg/min through a second venous cannula, started 2 min before image acquisition. Rest perfusion images were obtained 15 min after stress imaging using identical scanning parameters and slice location. Cardiac function was assessed in between stress and rest perfusion with steady-state free-precession cine imaging. Late gadolinium enhancement (LGE) was performed 12 to 15 min after rest perfusion using a 2-dimensional segmented inversion-recovery gradient-echo pulse sequence.

CMR IMAGE ANALYSIS. Perfusion images were analyzed using dedicated research software (MASS version 2017-Exp, Leiden, the Netherlands). Cine and LGE images were analyzed using commercially available software (QMASS version 7.6, Medis, Leiden, the Netherlands). The myocardium was divided into 16 segments (true apex not included), which were allocated to vascular territories using anatomic information from the invasive angiogram. In addition to this modified segmentation, myocardial segments were allocated to vascular territories according to the standard segmentation model of the American Heart Association (19). Visual analysis of perfusion images was performed by consensus of 2 expert observers (R.N. and R.L.). First, quality of the images was graded as 0 (not assessable), 1 (poor), 2 (moderate), or 3 (good). Next, the occurrence of splenic switch-off was visually assessed by comparing the rest and stress perfusion images. Thereafter, perfusion was scored per segment as 0 (normal), 1 (mildly abnormal), or 2 (severely abnormal). LGE images were reviewed alongside perfusion images to evaluate hyperenhancement. The transmural extent of hyperenhancement was scored per segment as: 0 (absent), 1 (1% to 25%), 2 (26% to 50%), 3 (51% to 75%), and 4 (>75%). Summation scores were calculated on a per-vessel and per-patient basis by adding the perfusion scores of the individual segments. Because the region of hyperenhancement resulting from the recent STEMI may exceed the segments allocated to the culprit (20), all hyperenhanced segments were excluded provided that the hyperenhancement was clearly related to the index event. Segments with hyperenhancement according to a nonischemic pattern were also excluded (21); thus, segments in nonculprit vascular territories with incidental hyperenhancement were only included if the hyperenhancement was clearly unrelated to the index event and demonstrated an ischemic pattern. Semi- and fully quantitative analysis of perfusion were performed by a single observer (H.E.), supervised by a second observer (R.N.). Endocardial and epicardial contours were manually drawn on the basal, mid, and apical slices of both the stress and rest perfusion series. A region of interest was placed in the blood pool of the perfusion series obtained for the arterial input function. Semiquantitative analysis of myocardial perfusion was performed by calculating the relative upslope of the signal intensity time curve, as described previously (3). Fully quantitative analysis was performed by Fermi function constrained deconvolution of the signal intensity time curves according to previously described methods (4). Myocardial flow reserve (MFR) was calculated as the ratio of stress to rest perfusion parameters. Perfusion in myocardium subtended by a nonculprit vessel was calculated by averaging 2 adjacent segments with the lowest perfusion values in the vascular territory of the nonculprit vessel. In an additional analysis, perfusion was calculated by averaging the entire vascular territory of the nonculprit vessel. Remote myocardium was defined as the myocardial segments vascularized by a nonculprit vessel with <50% diameter stenosis. LV end-diastolic volume, end-systolic volume, and ejection fraction were calculated from the cine images. Infarct size was calculated from the LGE images using the full width at half maximum method. Additionally, the LGE images were evaluated for presence of microvascular obstruction. All CMR analyses were performed blinded to clinical information, coronary angiography results, and data obtained from invasive measurements.

FOLLOW-UP INVASIVE CORONARY ANGIOGRAPHY AND PHYSIOLOGICAL INTERROGATION. A guiding catheter was advanced into the coronary ostium of the stenotic nonculprit vessel. After regular coronary

FIGURE 1 Flowchart of Study Population

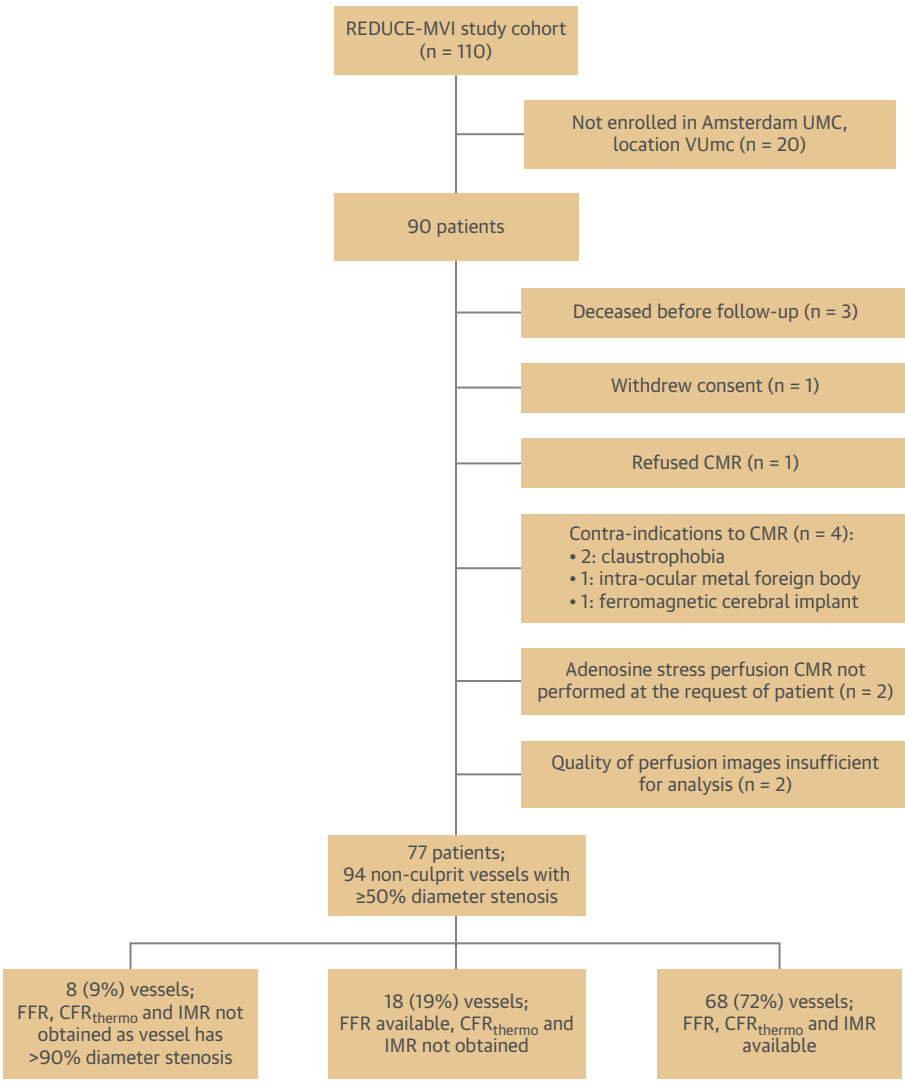

CFR$_{thermo}$ = thermodilution derived coronary flow reserve; CMR = cardiac magnetic resonance; FFR = fractional flow reserve; IMR = index of microcirculatory resistance.

angiography, 200 μg of nitrates were administered as an intracoronary bolus. A pressure/temperature sensor-tipped guidewire (PressureWire X wired, Abbott, Chicago, Illinois) was placed in the distal part of the stenotic nonculprit vessel and connected to the RadiAnalyzer interface (Abbott). Next, hyperemia was induced through intravenous infusion of adenosine using the same protocol as applied during CMR. FFR was obtained after at least 2 min of infusion. Lesions with FFR ≤0.80 were regarded as hemodynamically obstructive. Lesions with ≥90% diameter stenosis were not subjected to physiological interrogation and were also regarded as hemodynamically obstructive. In a subset of vessels, thermodilution derived coronary flow reserve (CFR$_{thermo}$) and index of microcirculatory resistance (IMR) were determined as described previously (22,23). Abnormal CFR was defined as CFR ≤2.0. IMR was considered abnormal if ≥25 U. In all patients, the angiogram was visually assessed to identify collateral pathways. Collateral vessels were graded according to the collateral connection score (24) and the Rentrop and Cohen classification (25).

TABLE 1 Baseline Characteristics (N = 77)

Age (yrs)	60 ± 10
Male	68 (86.0)
Body mass index (kg/m^2)	28 ± 4
Risk factors	
Family history of CAD	27 (35.0)
Hypertension	23 (30.0)
Hypercholesterolemia	14 (18.0)
Diabetes mellitus	7 (9.0)
Smoking	42 (55.0)
Symptom-to-balloon time (min)	182 [114-400]
Killip class on admission	
I	73 (95.0)
II	1 (1.0)
III	1 (1.0)
IV	2 (3.0)
GRACE risk score	114 ± 22
TIMI risk score	2.7 ± 1.7
Medication at discharge	
ACE inhibitor or ATII antagonist	69 (90.0)
Aspirin	77 (100.0)
Beta-blocker	72 (94.0)
P2Y12 inhibitor	77 (100.0)
Statin	76 (99.0)

Values are mean ± SD, n (%), or median [interquartile range].

ACE = angiotensin-converting enzyme; ATII = angiotensin II receptor; CAD = coronary artery disease; GRACE = Global Registry of Acute Coronary Events; TIMI = Thrombolysis In Myocardial Infarction.

TABLE 2 Angiographic and CMR Characteristics (N = 77)

Timing of follow-up CMR and ICA	
Time between pPCI and CMR (days)	30 [28-33]
Time between pPCI and follow-up ICA (days)	31 [29-34]
Time between CMR and follow-up ICA (days)	0 [0-1]
Infarct-related artery	
LAD/LCx/RCA	32/25/20
Nonculprit lesion location	
LAD/LCx/RCA	35/33/26
Multivessel disease	
Two vessel	60 (78)
Triple vessel	17 (22.0)
Nonculprit vessels	
FFR	0.87 [0.75-0.92]
With FFR ≤0.80	36 (38.0)
With FFR >0.80	58 (62.0)
LV volumes and function	
LV ED volume (ml/m^2)	91 ± 16
LV ES volume (ml/m^2)	42 ± 15
LV EF (%)	56 ± 8
Infarct size (% of LV)	5.6 [2.7-10.1]
Microvascular obstruction	2 (3.0)

Values are median [interquartile range], n, n (%), or mean ± SD.

CMR = cardiac magnetic resonance; ED = end-diastolic; EF = ejection fraction; ES = end-systolic; FFR = fractional flow reserve; ICA = invasive coronary angiography; LAD = left anterior descending artery; LCx = left circumflex artery; LV = left ventricle; pPCI = primary percutaneous coronary intervention; RCA = right coronary artery.

STATISTICAL ANALYSIS. Continuous variables are presented as mean ± SD or median (interquartile range), whereas categorical variables are expressed as frequency with percentage. Rest and stress perfusion were compared using the paired sample Student's *t*-test. Means of perfusion indexes were compared between vessels using a mixed linear model with a random effect for patient. Receiver-operatoring characteristic (ROC) curve analysis and the Youden index were used to define optimal cutoff values. Comparison of ROC curves was performed by using the method of DeLong. The McNemar test was used to compare sensitivity and specificity between perfusion indexes. All statistical tests were 2-tailed and a p value of <0.05 was considered statistically significant. Statistical analysis was done with SPSS version 22 for Windows (IBM, Armonk, New York).

RESULTS

PATIENT CHARACTERISTICS. Stress perfusion CMR was successfully performed in 77 of the 90 patients enrolled in the Amsterdam UMC, location VUmc (Figure 1). Baseline characteristics of the study cohort are listed in Table 1. Table 2 displays the angiographic and CMR characteristics. Follow-up CMR and invasive assessment were performed on the same day in 53 (69%) patients. Figure 2 depicts a case of concordance between CMR and FFR. In the 77 patients, 94 nonculprit vessels had ≥50% diameter stenosis and were used for analysis. Hemodynamically obstructive nonculprit lesions were present in 36 (38%) vessels of 31 (40%) patients. Collaterals pathways were identified in 5 (6%) patients (details listed in Supplemental Table 1). At follow-up, angina burden of the patient cohort was low, with mean SAQ scores of 84 ± 19 for physical limitation, 90 ± 16 for angina frequency, and 84 ± 28 for angina stability. LGE images revealed residual microvascular obstruction in 2 (3%) patients. Furthermore, incidental hyperenhancement in nonculprit vascular territories was observed in 6 segments of 3 vascular territories in 3 (4%) patients. In all 3 patients, the incidental hyperenhancement had an ischemic pattern and was clearly unrelated to the index event.

VISUAL ANALYSIS. The calculated summed stress scores ranged from 0 to 14. ROC curve analysis revealed an area under the curve (AUC) of 0.74 (95% confidence interval [CI]: 0.62 to 0.83) for visual analysis to detect hemodynamically obstructive

FIGURE 2 Case Example

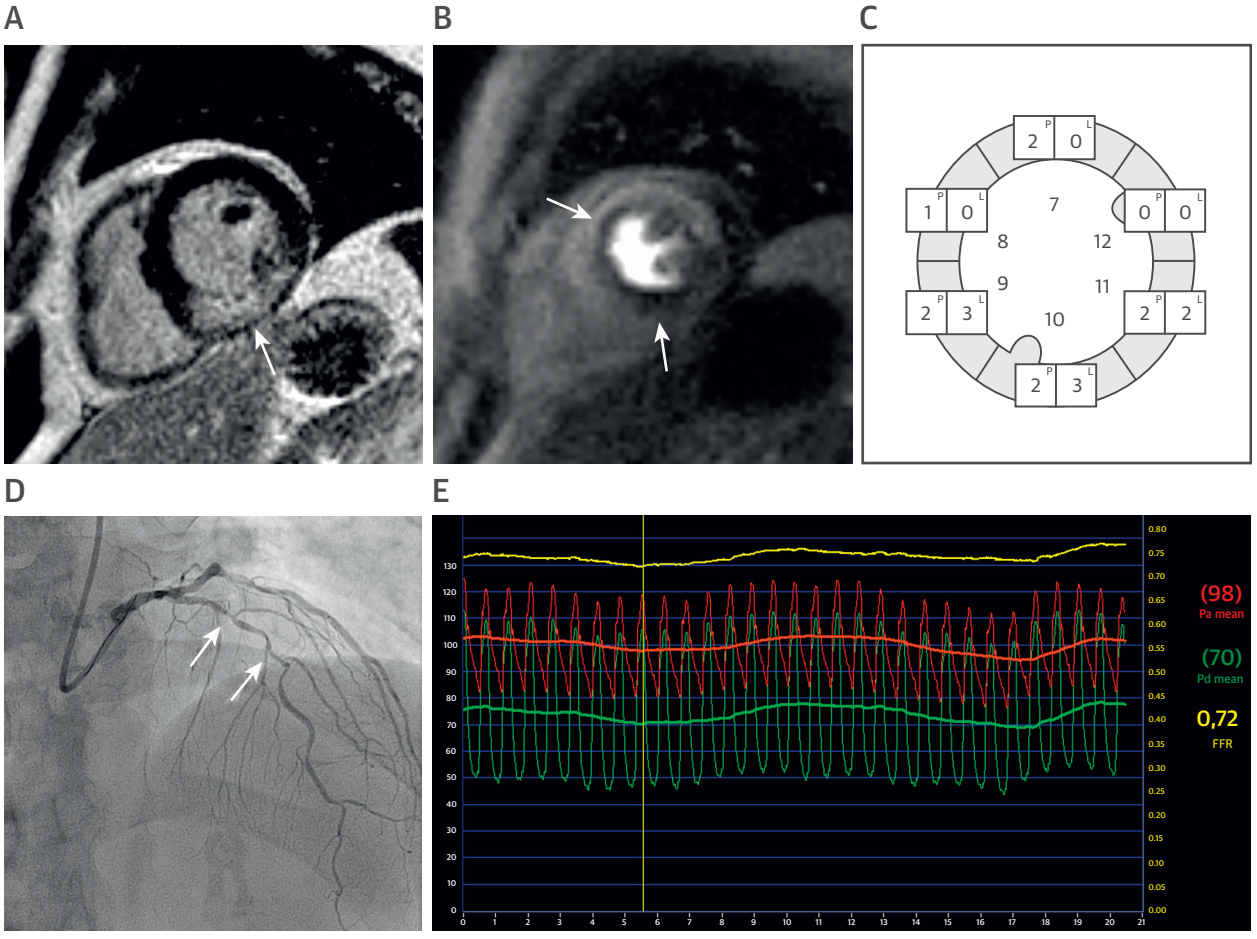

Short-axis images **(A and B)** on the mid-level acquired 1 month after acute myocardial infarction due to occlusion of the RCA. **(A)** The LGE image shows hyperenhancement of the inferior wall. **(B)** Stress perfusion imaging reveals hypoperfusion in the vascular territory of the RCA, but also in the territory of the LAD. Presence of perfusion abnormalities and LGE are scored for each segment (**C**, only the results of the current slice are shown). In the scoring sheet, the **left boxes** indicate the perfusion scores and the **right boxes** indicate the hyperenhancement scores. For the mid-slice of this patient, a summed stress score of 2 + 1 = 3 is calculated. Segments 9 to 11 are excluded from summation because the hyperenhancement in these segments is clearly related to the index event. **(D)** Invasive angiography demonstrates intermediate stenosis of the LAD, which is confirmed as **(E)** hemodynamically obstructive after measurement of FFR. LAD = left anterior descending artery; LGE = late gadolinium enhancement; RCA = right coronary artery; other abbreviation as in Figure 1.

nonculprit lesions on a per-patient level (**Figure 3**, top), with an optimal cutoff of ≥1. Using this cutoff, visual analysis achieved a per-patient sensitivity of 73% and a specificity of 70% (**Table 3**, left column). Lowering the FFR threshold from 0.80 to 0.75 resulted in an AUC of 0.76 (95% CI: 0.64 to 0.89) for summed stress scores (Supplemental Table 2). Splenic switch-off was present in 72 (94%) patients. All 5 patients with absent splenic switch-off had negative CMR results, although FFR was ≤0.80 in 1 (20%) patient. The agreement between of CMR and FFR was unaltered by including only patients who demonstrated splenic switch-off (Supplemental Figure 1).

SEMIQUANTITATIVE ANALYSIS. The relative upslope of the stress signal intensity time curve (stress rel upslope) and relative upslope derived flow reserve (MFR rel upslope) were significantly lower in myocardium supplied by stenotic nonculprit vessels with FFR ≤0.80 compared with stenotic nonculprit vessels with FFR >0.80 (10.0 ± 3% vs. 8.6 ± 2%; p = 0.04 for stress rel upslope and 1.7 ± 0.6 vs. 1.4 ± 0.5; p = 0.009 for MFR rel upslope). ROC curve analysis revealed an AUC of 0.66 (95% CI: 0.54 to

FIGURE 3 **Diagnostic Performance of Cardiac Magnetic Resonance**

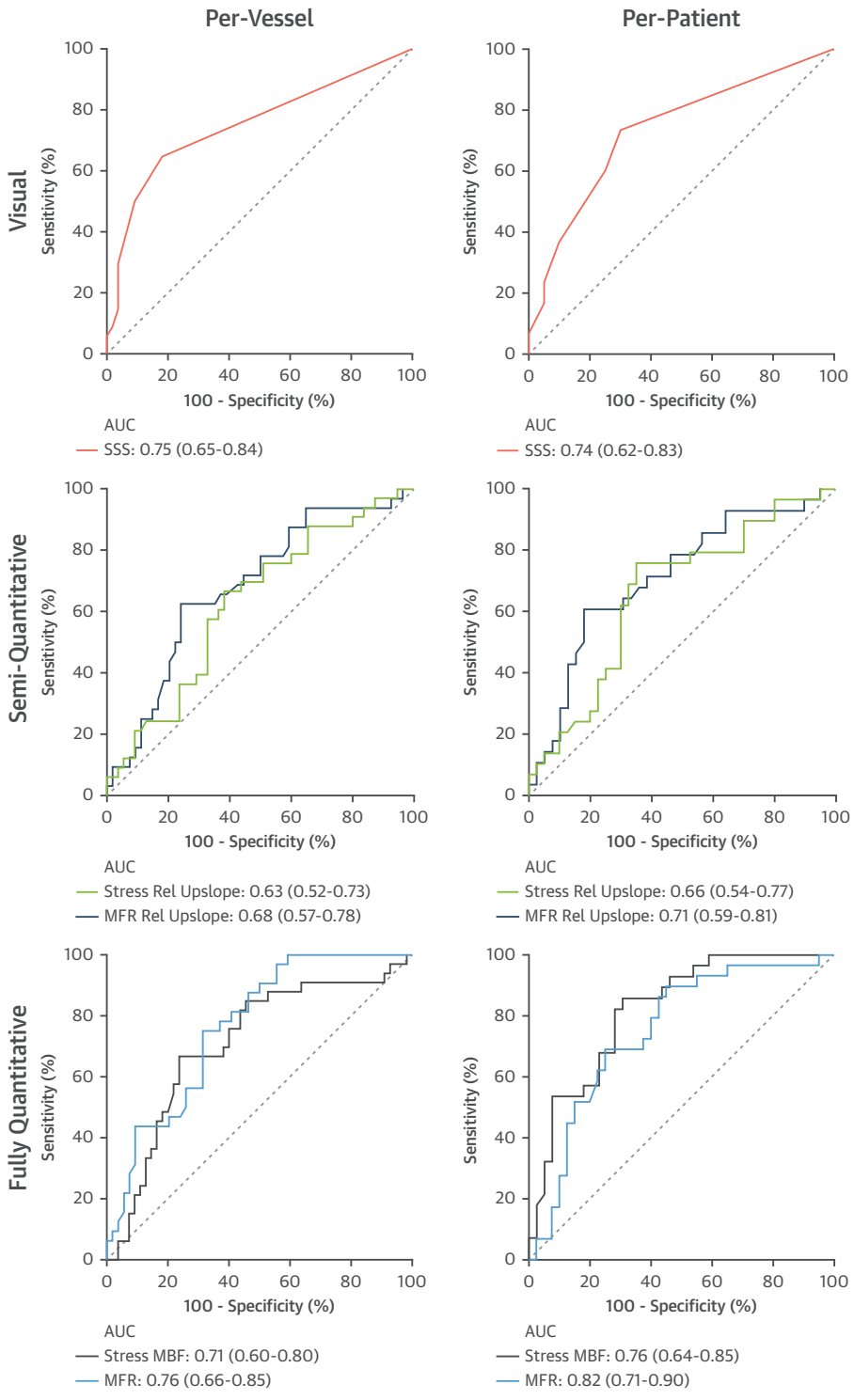

ROC curves of **(top)** visual, **(middle)** semiquantitative, and **(bottom)** fully quantitative analysis for detecting nonculprit lesions with FFR ≤0.80 on a **(left)** per-vessel and **(right)** per-patient basis. AUC = area under the curve; MBF = myocardial blood flow; MFR = myocardial flow reserve; rel upslope = relative upslope of the signal intensity time curve; ROC = receiver-operating characteristic; SSS = summed stress score.

TABLE 3 Diagnostic Performance of CMR for Diagnosing Angiographically Significant Nonculprit Lesions With FFR ≤0.80

	Visual	Semiquantitative		Fully Quantitative	
	SSS	Stress rel upslope	MFR rel upslope	Stress MBF	MFR
Per vessel					
Sensitivity (%)	65 (47-80)	67 (48-82)	63 (44-79)	67 (48-82)	75 (57-89)
Specificity (%)	82 (69-91)	63 (49-76)	76 (62-87)	76 (63-87)	69 (55-80)
PPV (%)	69 (54-80)	52 (42-63)	61 (47-73)	63 (50-74)	59 (48-69)
NPV (%)	79 (70-86)	76 (65-84)	77 (68-85)	79 (70-86)	82 (72-90)
Accuracy (%)	75 (65-84)	64 (54-74)	71 (60-80)	73 (62-82)	71 (60-80)
Per patient					
Sensitivity (%)	73 (54-88)	76 (56-90)	61 (41-79)	69 (49-85)	82 (63-94)
Specificity (%)	70 (54-83)	65 (49-79)	83 (68-93)	77 (61-88)	71 (55-84)
PPV (%)	63 (51-74)	59 (48-70)	71 (54-84)	67 (52-78)	66 (54-76)
NPV (%)	79 (67-88)	80 (67-89)	76 (66-83)	79 (68-87)	86 (73-93)
Accuracy (%)	71 (59-81)	69 (57-80)	74 (62-84)	74 (62-83)	76 (64-85)

Values are % (95% confidence interval). Semi- and fully quantitative perfusion in myocardium subtended by a nonculprit vessel was calculated by averaging 2 adjacent segments with the lowest perfusion values in the vascular territory of the nonculprit vessel. Vascular territories were defined using anatomical information from the invasive angiogram.

MBF = myocardial blood flow; MFR = myocardial flow reserve; NPV = negative predictive value; PPV = positive predictive value; rel upslope = relative upslope of the signal intensity time curve; SSS = summed stress score.

0.77) for stress rel upslope and 0.71 (95% CI: 0.59 to 0.81) for MFR rel upslope for diagnosing nonculprit vessels with FFR ≤0.80 on a per-patient basis (**Figure 3**, middle). The optimal cutoff values of stress rel upslope and MFR rel upslope for detecting hemodynamically obstructive nonculprit lesions were 9.1% and 1.4, respectively. Using these cutoff values, stress rel upslope achieved a per-patient sensitivity of 76% and a specificity of 65% (**Table 3**, central column). MFR rel upslope had similar diagnostic performance ($p = 0.50$), with a sensitivity of 61% and a specificity of 83%. When applying an FFR threshold of 0.75 instead of 0.80, ROC curve analysis displayed an AUC of 0.68 (95% CI: 0.54 to 0.81) for stress rel upslope and 0.75 (95% CI: 0.63 to 0.87) for MFR rel upslope (Supplemental Table 2).

FULLY QUANTITATIVE ANALYSIS. Mean MBF in remote myocardium was 1.11 ± 0.30 ml/min/g at rest and increased to 2.77 ± 0.76 ml/min/g during stress ($p < 0.001$), with a mean MFR of 2.84 ± 1.12. In myocardium vascularized by stenotic nonculprit vessels, rest MBF was 0.91 ± 0.28 ml/min/g and stress MBF was 2.18 ± 0.68 ml/min/g ($p < 0.001$), yielding a mean MFR of 2.05 ± 0.75. Stress MBF and MFR were significantly lower in myocardium vascularized by stenotic nonculprit vessels with FFR ≤0.80 compared with stenotic nonculprit vessels with FFR >0.80 (2.38 ± 0.69 ml/min/g vs 1.90 ± 0.59 ml/min/g; $p < 0.001$ for stress MBF and 2.31 ± 0.77 ml/min/g vs 1.61 ± 0.44 ml/min/g; $p < 0.001$ for MFR; **Central Illustration**). In contrast, rest MBF did not differ between stenotic nonculprit vessels with and without hemodynamically obstructive stenosis (0.91 ± 0.29 ml/min/g vs 0.93 ± 0.26 ml/min/g; $p = 0.77$). On a per-patient level, ROC curve analysis revealed an AUC of 0.76 (95% CI: 0.64 to 0.85) for stress MBF and 0.82 (95% CI: 0.71 to 0.90) for MFR (**Figure 3**, bottom). There was no difference in the diagnostic performance of stress MBF and MFR ($p = 0.50$). The optimal cutoff values for diagnosing nonculprit lesions with FFR ≤0.80 were 1.98 ml/min/g for stress MBF and 2.10 for MFR. Using these cutoff values, stress MBF and MFR, respectively, achieved per-patient sensitivities of 69% and 82%, and specificities of 77% and 71% (**Table 3**, right column). Lowering the FFR threshold from 0.80 to 0.75 resulted in an AUC of 0.74 (95% CI: 0.63 to 0.86) for stress MBF and 0.84 (95% CI: 0.74 to 0.93) for MFR (Supplemental Table 2).

COMPARISON BETWEEN VISUAL, SEMIQUANTITATIVE, AND FULLY QUANTITATIVE ANALYSIS. Visual, semiquantitative, and fully quantitative analysis yielded similar diagnostic performances (all $p > 0.05$). Sensitivity and specificity also did not significantly differ between fully quantitative and visual analysis (all $p > 0.05$) (**Table 3**). Supplemental Table 3 lists the diagnostic performance of CMR using the standard American Heart Association segmentation model. Supplemental Table 4 lists the diagnostic performance of CMR using the average myocardial perfusion in the vascular territory of the nonculprit vessel. In both models, semi- and fully quantitative analysis demonstrated similar diagnostic performance (all $p > 0.05$).

INFLUENCE OF MICROVASCULAR FUNCTION ON DIAGNOSTIC PERFORMANCE. CFR_{thermo} and IMR were obtained in 68 (72%) vessels of 66 (86%)

CENTRAL ILLUSTRATION **Fully Quantitative Perfusion in Vascular Territories of Nonculprit Vessels**

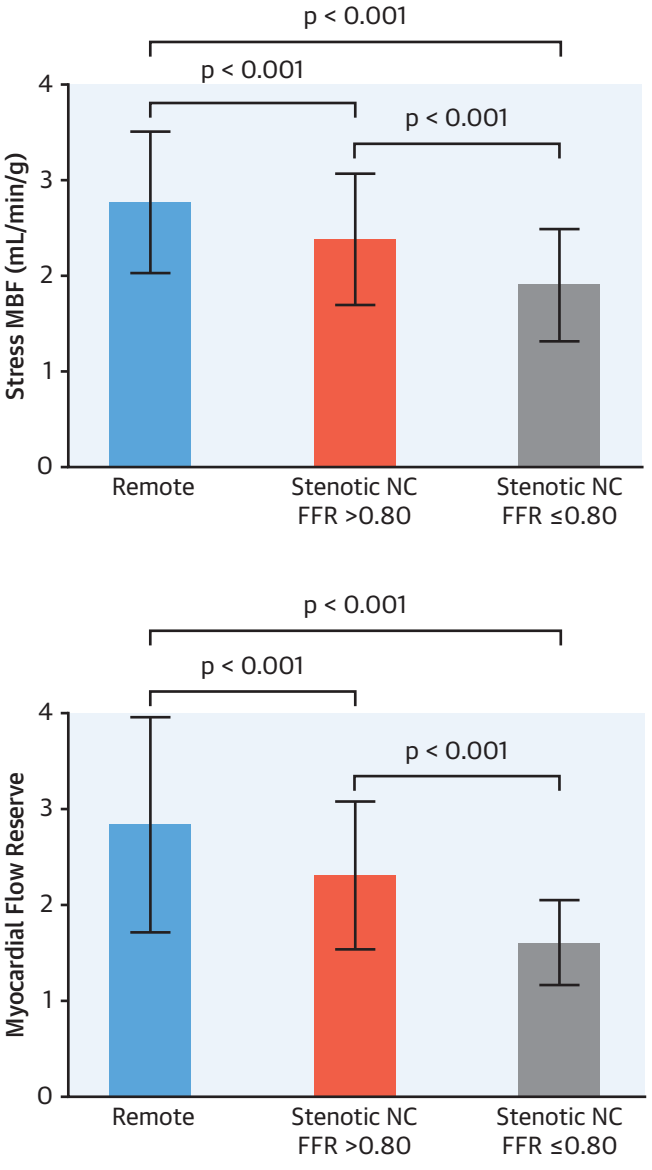

Everaars, H. et al. J Am Coll Cardiol Img. 2020;13(3):715-28.

Stress MBF and MFR in myocardium supplied by stenotic non-culprit vessels and in myocardium supplied by vessels without significant angiographic stenosis (remote). Stenotic vessels are further stratified according to FFR. NC = nonculprit vessel; other abbreviations as in Figures 1 and 3.

patients. CFR_{thermo} was ≤2.0 in 10 (15%) vessels, 7 (70%) of which had an FFR >0.80. IMR was ≥25 in 15 (22%) vessels, 13 (87%) of which had FFR >0.80. Figure 4 displays the diagnostic performance of CMR for diagnosing hemodynamically obstructive nonculprit when only vessels with CFR_{thermo} >2 or IMR <25 U are included. The agreement between CMR and FFR was unaltered in vessels with normal CFR_{thermo} or normal IMR.

DISCUSSION

This is the first study to investigate the agreement between CMR and FFR in the evaluation of

FIGURE 4 Diagnostic Performance Of CMR In Patients With Normal Microvascular Function

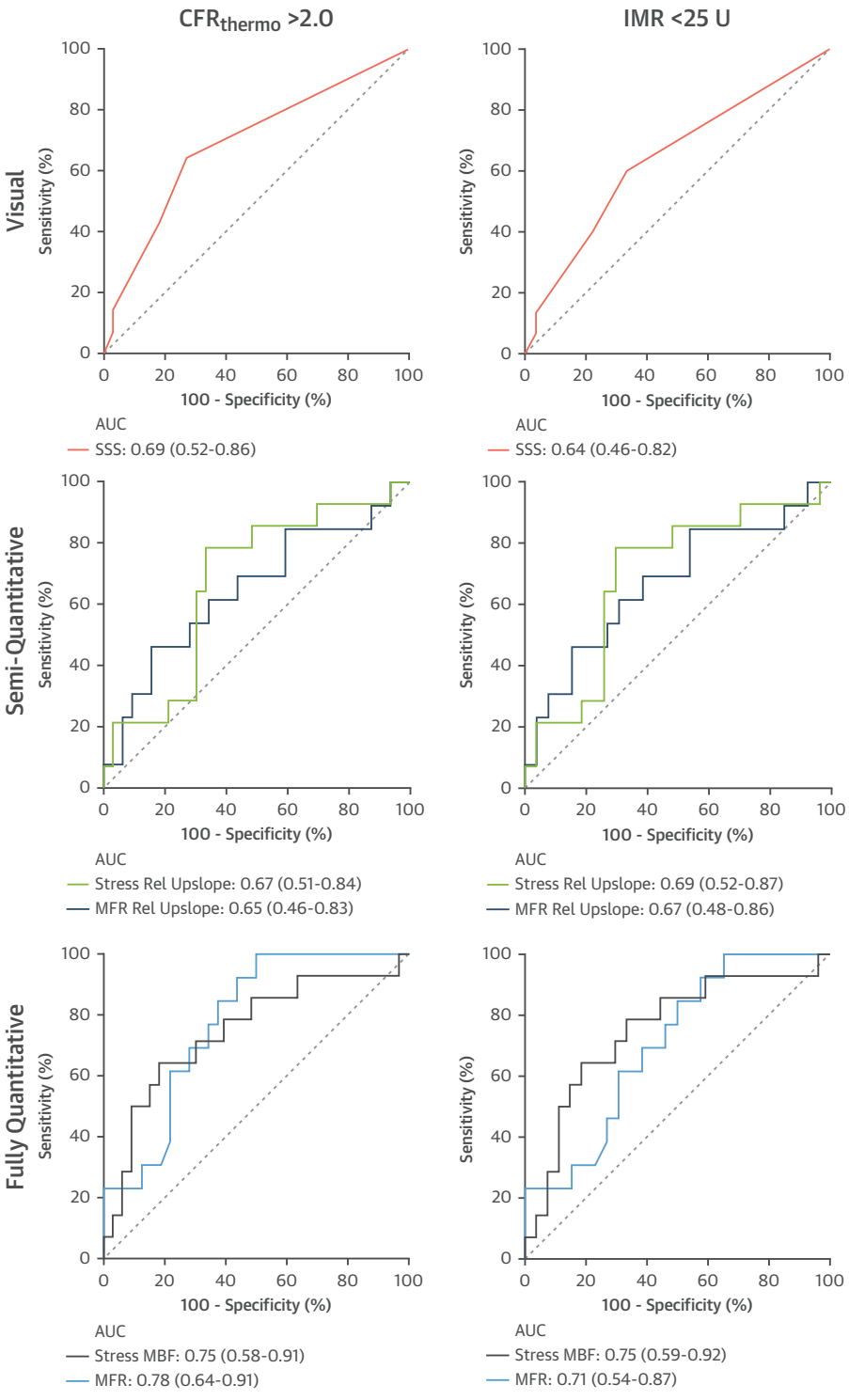

(Top) ROC curves of visual, **(middle)** semiquantitative, and **(bottom)** fully quantitative analysis for diagnosing nonculprit lesions with FFR ≤0.80 including only vessels with (left) CFR$_{thermo}$ >2 or (right)IMR <25 U. Abbreviations as in Figures 1 and 3.

nonculprit lesions in reperfused patients with STEMI with multivessel disease. The main findings are summarized as follows: 1) CMR and FFR have moderate-good agreement in the evaluation of nonculprit lesions after STEMI; and 2) fully quantitative analysis of myocardial perfusion is not superior to semiquantitative or visual analysis.

AGREEMENT BETWEEN CMR AND FFR. Several studies have investigated the diagnostic value of CMR in stable CAD. Notably, the multicenter CE-MARC (Cardiovascular Magnetic Resonance and Single-Photon Emission Computed Tomography for Diagnosis of Coronary Heart Disease) trial documented a sensitivity of 87% and specificity of 84% of CMR for diagnosing obstructive CAD (26). In contrast to the high agreement reported in stable patients with suspected CAD, we observed a lower concordance between CMR and FFR in the evaluation of nonculprit lesions after STEMI. This may be partially explained by selection, although the applied selection is not uncommon because patients with STEMI with multivessel disease are currently more often referred for FFR-guided revascularization of the nonculprit lesions. In our study, only vessels with ≥50% diameter stenosis were included for analysis because nonculprit vessels without significant angiographic stenosis can be deferred based on the angiogram obtained during primary intervention. Including only vessels with angiographic stenosis will inevitably result in a lower agreement with FFR because the concordance between 2 continuous variables decreases when the investigated values are close to the cutoff. Selection can therefore influence the agreement between any 2 techniques. For instance, [^{15}O]H_2O positron emission tomography, which is considered to be the gold standard for myocardial perfusion imaging, is reported to be concordant with FFR in 86% of cases (27). When only vessels with angiographic stenosis are included, the agreement drops to 72% (28), similar to our results. Second, hyperemic perfusion and FFR show physiological discordance in approximately 25% of cases (27), mainly because of varying degrees of microvascular dysfunction (29). After STEMI, microvascular dysfunction can be present either concomitantly or as a result of acute ischemic injury. Several studies have indicated that in STEMI acute microvascular dysfunction is not confined to the culprit area but also affects remote myocardium (30,31). Given a certain geometric stenosis, microvascular dysfunction limits maximal achievable blood flow resulting in lower hyperemic perfusion and elevated FFR. As the physiological disturbances resulting from the acute ischemic injury resolve over time, FFR decreases, whereas hyperemic MBF and MFR increase (31,32). The agreement between CMR and FFR observed in the present study therefore does not reflect failure of either technique but rather underscores that FFR represents a different measure of physiology than hyperemic MBF and MFR. It is important to note, however, that ischemia is driven by reductions in flow, not changes in coronary pressure (33). One could therefore argue that in combined epicardial and microvascular disease, hyperemic perfusion more accurately discerns diseased vessels inducing ischemia than FFR.

OPTIMAL TREATMENT STRATEGY FOR NONCULPRIT LESIONS IN STEMI. Patients with STEMI with multivessel disease represent a complex patient group. A wide spectrum of treatment options is available for nonculprit lesions, ranging from complete multivessel revascularization during primary intervention to a conservative strategy of optimal medical therapy alone. Four large randomized trials have thus far compared preventive revascularization to a conservative approach (12,34–36). All demonstrated lower incidences of major adverse cardiovascular events in the preventive revascularization group, indicating that optimal medical therapy alone does not suffice. Importantly, the results of these trials should not be interpreted as preventive revascularization being the optimal treatment strategy for nonculprit lesions after STEMI because no data exist demonstrating that noninvasive imaging is inferior. Previous studies have demonstrated that negative results of both CMR and FFR are associated with a low risk of events (2,37); however, the prognostic implications of discordancy between CMR and FFR are unknown. Although the present study demonstrates moderate-good agreement between CMR and FFR in the evaluation of nonculprit lesions after STEMI, it remains uncertain whether CMR-guided treatment of nonculprit lesions also translates into different outcome than FFR-guided revascularization. Interestingly, patients with STEMI with multivessel disease have a low angina burden during follow-up. In the present study, patients reported a mean SAQ score of 90 for angina frequency, which corresponds to chest discomfort experienced once a month or not at all. This is in line with findings from previous studies, which also reported that nonculprit lesions after STEMI rarely cause angina (12,34–36). Silent ischemia after myocardial infarction is nevertheless important to diagnose and treat. In the SWISSI II (Swiss Interventional Study on Silent Ischemia Type II) trial, patients with a previous myocardial infarction, documented ischemia, and angiographic stenosis

were randomly assigned to revascularization or optimal medical therapy (38). Revascularization was associated with a 56% reduction in cardiac events. Randomized trials comparing imaging guided treatment of nonculprit lesions to preventive revascularization, such as the ongoing iMODERN (iFR Guided Multi-vessel Revascularization During Percutaneous Coronary Intervention for Acute Myocardial Infarction) trial (39), are thus eagerly warranted.

IS PERFUSION QUANTIFICATION WORTH THE EFFORT? In recent years, increased focus has been placed on absolute quantification of myocardial perfusion using CMR. Quantification holds several advantages over visual assessment. It is less dependent on the experience of the reader and does not require a myocardial region with normal perfusion for comparison. Mordini et al. (5) compared the diagnostic performances of fully quantitative, semiquantitative, and visual assessment and reported superiority of fully quantitative analysis over both visual and semiquantitative analysis. In contrast to the findings of Mordini et al. (5), 2 small studies found no benefits of quantification over visual assessment (6,7). In keeping with the results of these studies, a recently published substudy of the CE-MARC trial also reported similar diagnostic performance of quantitative and visual assessment (8). This could be in part because visual analysis already displayed excellent accuracy. In the present study, visual analysis had moderate agreement with FFR. Quantification nevertheless failed to demonstrate incremental value.

STUDY LIMITATIONS. The present report is a substudy of the REDUCE-MVI trial, which was powered to assess differences in IMR in the culprit vessel of patients with STEMI randomized to a maintenance therapy of ticagrelor or prasugrel. The current substudy may therefore be underpowered and the limited sample size may have resulted in a type II error in the comparative testing of AUC curves. In addition, the limited sample size hindered analysis on the diagnostic performance of CMR in patients with abnormal microvascular function, as defined by either CFR_{thermo} or IMR; however, the agreement between CMR and FFR in patients with STEMI with multivessel disease has never been reported which make the present data unique. Second, invasive measurements of FFR were used as reference. Although FFR is considered the gold standard for guiding revascularization in patients with stable CAD, it has not been established as such for the management of nonculprit lesions after STEMI. The results of the present study should therefore be interpreted with caution. Finally, collateral connections from and to stenotic nonculprit vessels may have influenced FFR measurements. In the present study, visual collateral vessels were identified in 5 patients. Collateral pathways of smaller size that are not visualized on coronary angiography may nonetheless have influenced the results.

CONCLUSIONS

CMR and FFR have moderate-good agreement in the evaluation of nonculprit lesions in reperfused patients with STEMI with multivessel disease. Fully quantitative analysis of myocardial perfusion is not superior to semiquantitative or visual analysis.

ADDRESS FOR CORRESPONDENCE: Dr. Robin Nijveldt, Amsterdam University Medical Center, location VUmc, Department of Cardiology, De Boelelaan 1117, 1081 HV, Amsterdam, the Netherlands. E-mail: robin@nijveldt.net.

PERSPECTIVES

COMPETENCY IN MEDICAL KNOWLEDGE: This single-center study demonstrated that in patients with STEMI with multivessel disease, CMR and FFR have moderate-good agreement in the assessment of nonculprit lesions. Fully quantitative, semiquantitative, and visual analysis showed equivalent diagnostic performances.

TRANSLATIONAL OUTLOOK 1: Neither CMR measurements of myocardial perfusion nor invasive measurements of FFR have been established as the optimal treatment strategy for nonculprit lesions after STEMI. Multicenter trials randomizing patients with STEMI with multivessel disease to a perfusion imaging guided strategy or an invasive physiology guided strategy are thus eagerly awaited.

TRANSLATIONAL OUTLOOK 2: Multicenter studies using invasive physiology as reference should answer the question if quantification of myocardial perfusion improves the diagnostic performance of CMR. Even if so, quantification of absolute MBF from perfusion CMR is currently a laborious, time-consuming process, in contrast to the more straightforward visual analysis. To implement perfusion quantification into the clinic, image acquisition and post-processing have to be accelerated and automated.

REFERENCES

1. Pletscher M, Walker S, Moschetti K, et al. Cost-effectiveness of functional cardiac imaging in the diagnostic work-up of coronary heart disease. Eur Heart J Qual Care Clin Outcomes 2016;2:201–7.

2. Greenwood JP, Herzog BA, Brown JM, et al. Prognostic value of cardiovascular magnetic resonance and single-photon emission computed tomography in suspected coronary heart disease: long-term follow-up of a prospective, diagnostic accuracy cohort study. Ann Intern Med 2016;165:1–9.

3. Nagel E, Klein C, Paetsch I, et al. Magnetic resonance perfusion measurements for the noninvasive detection of coronary artery disease. Circulation 2003;108:432–7.

4. Jerosch-Herold M, Swingen C, Seethamraju RT. Myocardial blood flow quantification with MRI by model-independent deconvolution. Med Phys 2002;29:886–97.

5. Mordini FE, Haddad T, Hsu L-Y, et al. Diagnostic accuracy of fully quantitative, semi-quantitative, and qualitative assessment of stress perfusion CMR compared to quantitative coronary angiography. J Am Coll Cardiol Intv 2014;7:14.

6. Patel AR, Antkowiak PF, Nandalur KR, et al. Assessment of advanced coronary artery disease: advantages of quantitative cardiac magnetic resonance perfusion analysis. J Am Coll Cardiol 2010;56:561–9.

7. Chiribiri A, Hautvast GL, Lockie T, et al. Assessment of coronary artery stenosis severity and location: quantitative analysis of transmural perfusion gradients by high-resolution MRI versus FFR. J Am Coll Cardiol Intv 2013;6:600–9.

8. Biglands JD, Ibraheem M, Magee DR, Radjenovic A, Plein S, Greenwood JP. Quantitative myocardial perfusion imaging versus visual analysis in diagnosing myocardial ischemia: a CE-MARC substudy. J Am Coll Cardiol Intv 2018;11:711–8.

9. Pijls NH, Fearon WF, Tonino PA, et al. Fractional flow reserve versus angiography for guiding percutaneous coronary intervention in patients with multivessel coronary artery disease: 2-year follow-up of the FAME (Fractional Flow Reserve Versus Angiography for Multivessel Evaluation) study. J Am Coll Cardiol 2010;56:177–84.

10. Danad I, Szymonifka J, Twisk JWR, et al. Diagnostic performance of cardiac imaging methods to diagnose ischaemia-causing coronary artery disease when directly compared with fractional flow reserve as a reference standard: a meta-analysis. Eur Heart J 2017;38:991–8.

11. Sorajja P, Gersh BJ, Cox DA, et al. Impact of multivessel disease on reperfusion success and clinical outcomes in patients undergoing primary percutaneous coronary intervention for acute myocardial infarction. Eur Heart J 2007;28:1709–16.

12. Wald DS, Morris JK, Wald NJ, et al. Randomized trial of preventive angioplasty in myocardial infarction. N Engl J Med 2013;369:1115–23.

13. van Leeuwen MA, van der Hoeven NW, Janssens GN, et al. Evaluation of microvascular injury in revascularized patients with ST elevation myocardial infarction treated with ticagrelor versus prasugrel: the REDUCE-MVI Trial. Circulation 2019;139:636–46.

14. O'Gara PT, Kishner FG, Ascheim DD, et al. 2013 ACCF/AHA guideline for the management of ST-elevation myocardial infarction: a report of the American College of Cardiology Foundation/American Heart Association Task Force on Practice Guidelines. J Am Coll Cardiol 2013;61:e78–140.

15. Spertus JA, Winder JA, Dewhurst TA, et al. Development and evaluation of the Seattle Angina Questionnaire: a new functional status measure for coronary artery disease. J Am Coll Cardiol 1995;25:333–41.

16. Gatehouse PD, Elkington AG, Ablitt NA, Yang GZ, Pennell DJ, Firmin DN. Accurate assessment of the arterial input function during high-dose myocardial perfusion cardiovascular magnetic resonance. J Magn Reson Imaging 2004;20:39–45.

17. Chefd'Hotel C, Hermosillo G, Faugeras O. Flows of diffeomorphisms for multimodal image registration. Proceedings IEEE International Symposium on Biomedical Imaging 2002:753–6.

18. Kremers FP, Hofman MB, Groothuis JG, et al. Improved correction of spatial inhomogeneities of surface coils in quantitative analysis of first-pass myocardial perfusion imaging. J Magn Reson Imaging 2010;31:227–33.

19. Cerqueira MD, Weissman NJ, Dilsizian V, et al. Standardized myocardial segmentation and nomenclature for tomographic imaging of the heart a statement for healthcare professionals from the cardiac imaging committee of the Council on Clinical Cardiology of the American Heart Association. Circulation 2002;105:539–42.

20. Ortiz-Perez JT, Rodriguez J, Meyers SN, Lee DC, Davidson C, Wu E. Correspondence between the 17-segment model and coronary arterial anatomy using contrast-enhanced cardiac magnetic resonance imaging. J Am Coll Cardiol Img 2008;1:282–93.

21. Patel AR, Kramer CM. Role of cardiac magnetic resonance in the diagnosis and prognosis of nonischemic cardiomyopathy. J Am Coll Cardiol Intv 2017;10:1180–93.

22. Fearon WF, Balsam LB, Farouque HM, et al. Novel index for invasively assessing the coronary microcirculation. Circulation 2003;107:3129–32.

23. Pijls NH, De Bruyne B, Smith L, et al. Coronary thermodilution to assess flow reserve: validation in humans. Circulation 2002;105:2482–6.

24. Werner GS, Ferrari M, Heinke S, et al. Angiographic assessment of collateral connections in comparison with invasively determined collateral function in chronic coronary occlusions. Circulation 2003;107:1972–7.

25. Rentrop KP, Cohen M, Blanke H, Phillips RA. Changes in collateral channel filling immediately after controlled coronary artery occlusion by an angioplasty balloon in human subjects. J Am Coll Cardiol 1985;5:587–92.

26. Greenwood JP, Maredia N, Younger JF, et al. Cardiovascular magnetic resonance and single-photon emission computed tomography for diagnosis of coronary heart disease (CE-MARC): a prospective trial. Lancet 2012;379:453–60.

27. Danad I, Uusitalo V, Kero T, et al. Quantitative assessment of myocardial perfusion in the detection of significant coronary artery disease: cutoff values and diagnostic accuracy of quantitative [(15)O]H2O PET imaging. J Am Coll Cardiol 2014;64:1464–75.

28. de Waard GA, Danad I, Petraco R, et al. Fractional flow reserve, instantaneous wave-free ratio, and resting Pd/Pa compared with [15O]H2O positron emission tomography myocardial perfusion imaging: a PACIFIC trial sub-study. Eur Heart J 2018;39:4072–81.

29. van de Hoef TP, van Lavieren MA, Damman P, et al. Physiological basis and long-term clinical outcome of discordance between fractional flow reserve and coronary flow velocity reserve in coronary stenoses of intermediate severity. Circ Cardiovasc Interv 2014;7:301–11.

30. Bax M, de Winter RJ, Koch KT, Schotborgh CE, Tijssen JG, Piek JJ. Time course of microvascular resistance of the infarct and noninfarct coronary artery following an anterior wall acute myocardial infarction. Am J Cardiol 2006;97:1131–6.

31. Uren NG, Crake T, Lefroy DC, de Silva R, Davies GJ, Maseri A. Reduced coronary vasodilator function in infarcted and normal myocardium after myocardial infarction. N Engl J Med 1994;331:222–7.

32. van der hoeven NW, Janssens GN, de Waard GA, et al. Temporal changes in coronary hyperemic and resting hemodynamic indices in non-culprit vessels of patients with ST-segment elevation myocardial infarction. JAMA Cardiol 2019;4:501–10.

33. Smalling RW, Kelley K, Kirkeeide RL, Fisher DJ. Regional myocardial function is not affected by severe coronary depressurization provided coronary blood flow is maintained. J Am Coll Cardiol 1985;5:948–55.

34. Engstrom T, Kelbaek H, Helqvist S, et al. Complete revascularisation versus treatment of the culprit lesion only in patients with ST-segment elevation myocardial infarction and multivessel disease (DANAMI-3-PRIMULTI): an open-label, randomised controlled trial. Lancet 2015;386:665–71.

35. Gershlick AH, Khan JN, Kelly DJ, et al. Randomized trial of complete versus lesion-only revascularization in patients undergoing primary percutaneous coronary intervention for STEMI and multivessel disease: the CvLPRIT trial. J Am Coll Cardiol 2015;65:963–72.

36. Smits PC, Abdel-Wahab M, Neumann FJ, et al. Fractional flow reserve-guided multivessel angioplasty in myocardial infarction. N Engl J Med 2017;376:1234–44.

37. Pijls NH, van Schaardenburgh P, Manoharan G, et al. Percutaneous coronary intervention of functionally nonsignificant stenosis: 5-year follow-up of the DEFER Study. J Am Coll Cardiol 2007;49:2105–11.

38. Erne P, Schoenenberger AW, Burckhardt D, et al. Effects of percutaneous coronary

interventions in silent ischemia after myocardial infarction: the SWISSI II randomized controlled trial. JAMA 2007;297:1985–91.

39. iFR Guided Multi-vessel Revascularization During Percutaneous Coronary Intervention for Acute Myocardial Infarction (iMODERN). ClinicalTrials.gov website. Available at: https://clinicaltrials.gov/ct2/show/NCT03298659. Accessed November 5, 2018.

KEY WORDS **acute myocardial infarction, cardiac magnetic resonance, fractional flow reserve, non-culprit lesions, quantitative myocardial perfusion**

APPENDIX **For supplemental tables and figures, please see the online version of this paper.**